Cholesterol binds to synaptophysin and is required for biogenesis of synaptic vesicles

Christoph Thiele*†#, Matthew J. Hannah*†‡, Falk Fahrenholz§ and Wieland B. Huttner*†¶

*Department of Neurobiology, University of Heidelberg, Im Neuenheimer Feld 364, D-69120 Heidelberg, Germany
†Max-Planck-Institute of Molecular Cell Biology and Genetics, Pfotenhauerstrasse 110, D-01307 Dresden, Germany
‡Present address: MRC Laboratory for Molecular Cell Biology, University College London, Gower Street, London WC1E 6BT, UK
§Department of Biochemistry, University of Mainz, Becherweg 30, D-55099 Mainz, Germany
#e-mail: Christoph_Thiele@hotmail.com
¶e-mail: whuttner@sun0.urz.uni-heidelberg.de

Here, to study lipid–protein interactions that contribute to the biogenesis of regulated secretory vesicles, we have developed new approaches by which to label proteins *in vivo*, using photoactivatable cholesterol and glycerophospholipids. We identify synaptophysin as a major specifically cholesterol-binding protein in PC12 cells and brain synaptic vesicles. Limited cholesterol depletion, which has little effect on total endocytic activity, blocks the biogenesis of synaptic-like microvesicles (SLMVs) from the plasma membrane. We propose that specific interactions between cholesterol and SLMV membrane proteins, such as synaptophysin, contribute to both the segregation of SLMV membrane constituents from plasma-membrane constituents, and the induction of synaptic-vesicle curvature.

Cellular membranes are dynamic assemblies consisting of lipids and proteins. They are subject to continuous turnover as a result of budding of membrane vesicles from donor membranes and the fusion of vesicles with acceptor membranes. These processes involve sorting of both proteins and lipids, which results in donor organelles and the vesicles derived from them having different protein and lipid compositions. Two mechanisms contribute to the sorting of membrane constituents during vesicle-mediated membrane turnover. One mechanism is the interplay between a cytosolic protein machinery and lipid-embedded transmembrane protein anchors[1]; the other takes advantage of lipid–lipid and lipid–protein interactions that mediate lateral self-assembly to form distinct membrane subdomains, which serve as sorting platforms[2–5].

Two approaches have been widely used to study lipid–protein interactions. One is the analysis of the binding of soluble proteins to liposomes of defined lipid composition. The other approach is the analysis of detergent-insoluble complexes (DICs) obtained by treatment of cells or membranes with weak detergents[6]. These DICs have a distinct lipid and protein composition[6] and are thought to resemble self-organized structures (membrane 'rafts'), present in the membrane before the detergent treatment, that have been proposed to be important units with respect to both protein function and membrane sorting and traffic[3].

Although both approaches have proven useful for investigating various questions, they also have severe drawbacks. First, both are *in vitro* methods, and any interaction detected by them needs a critical evaluation for *in vivo* relevance. Second, the use of detergents for DIC preparation is a source of concern, as detergents tend to break hydrophobic lipid–protein interactions. Hence, although the presence of a protein in a DIC suggests (but does not prove) its interaction with cholesterol and/or sphingolipids, its absence cannot be taken as evidence for the lack of such an interaction. Third, analysis of DICs is not suitable to detect interactions of membrane proteins with glycerophospholipids.

An alternative approach by which to study lipid–protein interaction is photoaffinity labelling using photoactivatable radioactive lipids. Photoactivatable glycerophospholipids[7,8] and cholesterol derivatives[8] have previously been used to study model systems such as (proteo)liposomes[7] and purified, soluble lipid-binding proteins[9,10], but not for systematic screening for proteins that specifically interact with certain lipids in eukaryotic cells *in vivo*.

Here we describe a method for *in vivo* photoaffinity labelling that uses a new derivative of cholesterol and *in vivo*-generated photoactivatable radioactive glycerophospholipids. This approach allowed us to identify the specific interaction of cholesterol with membrane proteins of SLMVs in neuroendocrine cells. We found that the assembly of membrane proteins and lipids to form SLMVs was dependent on cellular cholesterol levels, showing the relevance of this interaction to membrane traffic.

Results

Synthesis and characterization of photocholesterol. We synthesized a photoactivatable analogue of cholesterol, refered to as photocholesterol; this analogue lacks the Δ5 double bond and the hydrogen at C-6, which are replaced by the photoactivatable diazirine ring (Fig. 1a). To obtain radioactively labelled photocholesterol, we oxidized unlabelled photocholesterol to the 3-keto compound 2 (see Methods) and then reduced the compound using tritiated sodium borohydride, yielding [^{3}H]photocholesterol (Fig. 1a) and its 3α-epimer (data not shown). [^{3}H]Photocholesterol and its 3α-epimer were subjected to enzymatic oxidation using cholesterol oxidase, which is specific for the 3β conformation of cholesterol and some other sterols. Only [^{3}H]photocholesterol, but not its 3α-epimer, was oxidized (Fig. 2a), showing that the hydroxyl group was in the correct (β) conformation and that photocholesterol shared overall conformational similarity with cholesterol.

Interaction of photocholesterol with proteins and lipids *in vitro*. To demonstrate the suitability of photocholesterol labelling to identify cholesterol-binding proteins, we studied the interaction of photocholesterol with known cholesterol-interacting partners. Cholesterol in the plasma is preferentially incorporated into high-density lipoproteins (HDLs) and low-density lipoproteins (LDLs), whose major protein components are apolipoprotein A1 and apolipoprotein B, respectively. Upon photoaffinity labelling of human plasma with [^{3}H]photocholesterol, we identified the major labelled bands as apolipoprotein A1 and apolipoprotein B by immunoprecipitation (Fig. 2b). Albumin, which has a strong tendency to interact nonspecifically with hydrophobic compounds, was not labelled.

Cholesterol also interacts specifically with other lipids[3], as

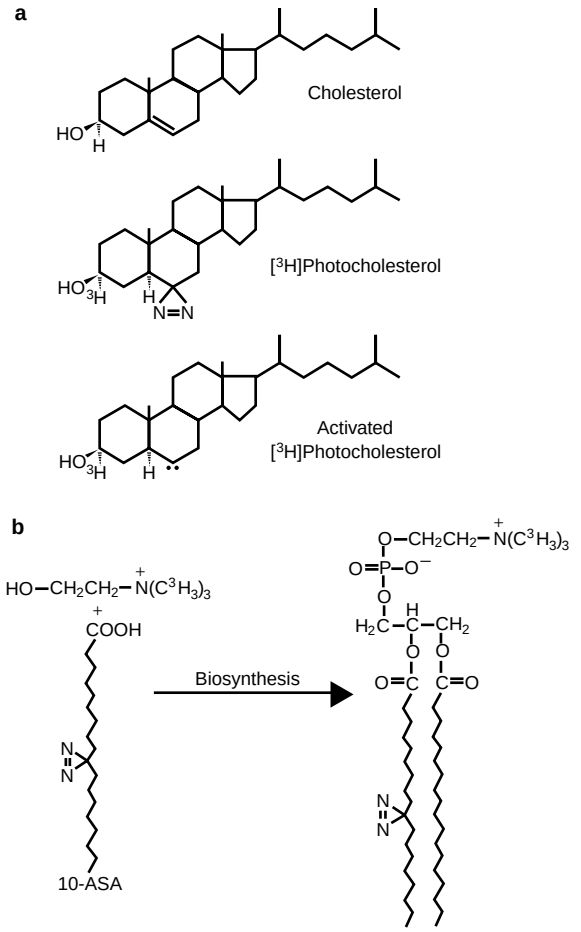

Figure 1 **Photoactivatable lipids: [^{3}H]photocholesterol and [^{3}H]photophosphatidylcholine. a**, Structures of cholesterol, the photoactivatable cholesterol analogue [^{3}H]photocholesterol, and [^{3}H]photocholesterol after activation by ultraviolet light. **b**, Biosynthetic generation of photoactivatable [^{3}H]photophosphatidylcholine from 10-azi-stearic acid (10-ASA) and [^{3}H]choline. The location of 10-ASA at position 2 of the glycerol backbone is hypothetical; location at position 1, or 1 and 2, is also possible.

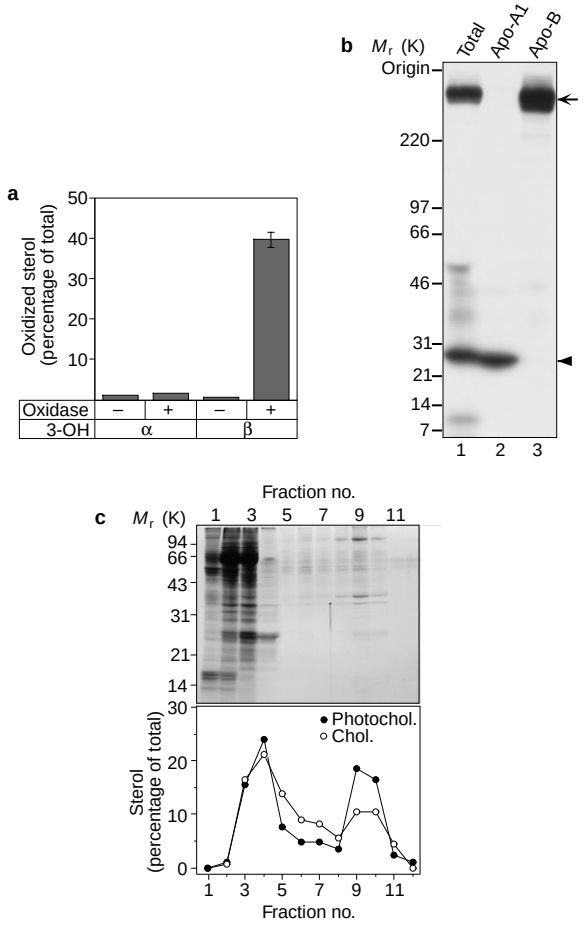

Figure 2 **Characterization of photocholesterol interactions with proteins and lipids. a**, Photocholesterol but not its 3α-epimer is a substrate for cholesterol oxidase. [^{3}H]Photocholesterol (3-OH β) and its 3α-epimer (3-OH α) were incubated in the absence or presence of cholesterol oxidase. The amount of oxidized sterol is expressed as a percentage of the total amount of sterol (sum of oxidized plus non-oxidized sterol). Data represent means±range of duplicate determinations. **b**, Photocholesterol labels cholesterol-binding proteins in human plasma. Human plasma was photolabelled with [^{3}H]photocholesterol, and apolipoproteins were immunoprecipitated. Lane 1, 1/12 of total labelled sample; lanes 2 and 3, 5/12 of labelled sample immunoprecipitated using antisera against apolipoprotein A1 (apo-A1, lane 2) or apolipoprotein B (apo-B, lane 3). Arrow, apolipoprotein B; arrowhead, apolipoprotein A1. Note the absence of photolabelled albumin (lane 1, M_r 66K). **c**, Photocholesterol, like cholesterol, partitions into detergent-insoluble complexes (DICs). Bovine chromaffin granule membranes were loaded for 1 h at 4 °C with [^{3}H]photocholesterol and lysed in 1% Triton X-100 at 4 °C. DICs were floated on a sucrose gradient. Top, SDS–PAGE/CBB staining of the gradient fractions. Bottom, distribution of [^{3}H]photocholesterol and cholesterol in the gradient fractions as determined by scintillation counting and quantitative TLC, respectively. The amount of the two sterols in each gradient fraction is expressed as a percentage of that found in the total gradient. Fraction 1, bottom of the gradient; fraction 12, top of the gradient. The peak of floating DICs is in fractions 9 and 10.

reflected by the formation of DICs upon detergent treatment of membranes rich in cholesterol and sphingolipids[6]. The membranes of bovine chromaffin granules form DICs upon treatment with Triton X-100; these DICs can be isolated using flotation in a sucrose gradient[6] (Fig. 2c). These DICs are enriched in cholesterol, sphingomyelin and a specific subset of proteins, most prominently the subunits of the vacuolar proton ATPase[11] (Fig. 2c, top; C.T. and W.B.H., unpublished observations). Upon incubation with bovine chromaffin granule membranes, [^{3}H]photocholesterol also incorporated into DICs (Fig. 2c, bottom). This indicates that [^{3}H]photocholesterol and cholesterol may undergo similar lateral interactions with other membrane constituents (most likely sphingolipids).

Lipid photaffinity labelling of membrane proteins *in vivo*. To investigate the suitability of [^{3}H]photocholesterol to label cholesterol-interacting partners *in vivo*, we performed photoaffinity labelling of MDCK cells. These cells contain the integral membrane protein caveolin/VIP21 (ref. 12), which binds cholesterol *in vitro*[13] and is assumed to do so *in vivo*[14], although experimental evidence for an *in vivo* interaction is lacking. Specific labelling of caveolin/VIP21 by [^{3}H]photocholesterol in live MDCK cells would provide such *in vivo* evidence, which in turn could be taken as an indication that [^{3}H]photocholesterol is suitable to detect membrane proteins that interact with cholesterol *in vivo*.

For photoaffinity-labelling experiments, MDCK cells were grown for 16 h in medium containing [^{3}H]photocholesterol complexed to methyl-β-cyclodextrin (MβCD). Metabolism of [^{3}H]photocholesterol by the cells was negligible (Fig. 3a). Hence, labelling of proteins upon ultraviolet irradiation would be attributable to the covalent incorporation of [^{3}H]photocholesterol rather than incorporation of a metabolite. After irradiation of the cells with ultraviolet light, several proteins incorporated radioactivity (Fig. 3b, lane 1). Labelling of proteins was dependent on ultraviolet irradiation

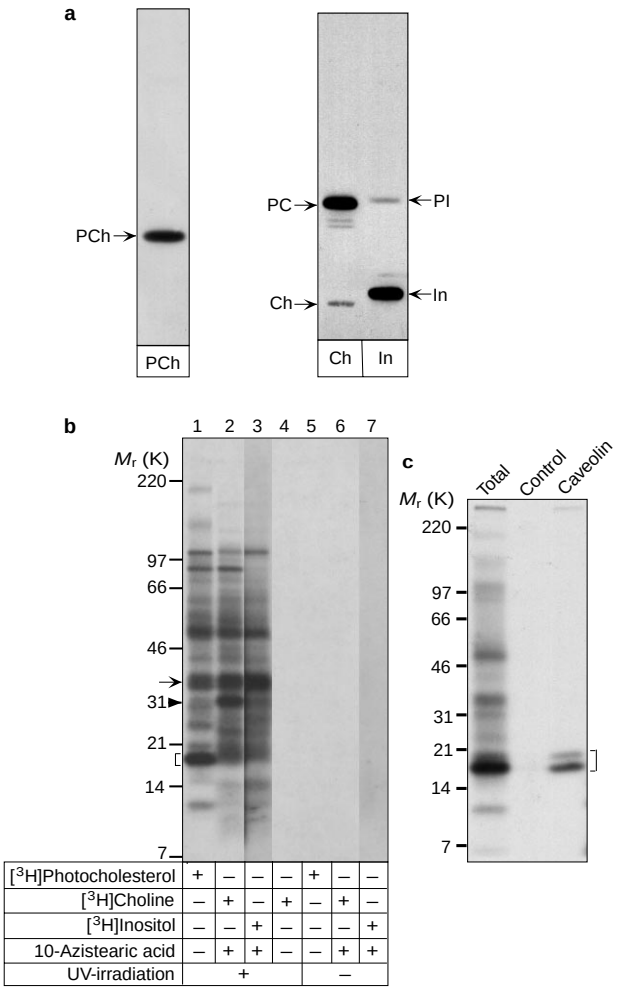

Figure 3 **Photoaffinity labelling of MDCK cells with photoactivatable lipids reveals specific binding of photocholesterol to caveolin/VIP21 *in vivo*.** **a**, TLC analysis of radioactive photoactivatable lipids. MDCK cells were grown in the presence of [^{3}H]photocholesterol (PCh, incubation time 16h), 10-ASA plus [^{3}H]choline (Ch, 20h), or 10-ASA plus [^{3}H]inositol (In, 20h). Detergent extracts were resolved on TLC plates followed by fluorography. The positions of co-migrating standards (PC, phosphatidylcholine; PI, phosphatidylinositol) are denoted by arrows. **b**, Distinct sets of proteins are labelled by different photoactivatable lipids. MDCK cells were grown in the presence of [^{3}H]photocholesterol (lanes 1, 5), 10-ASA plus [^{3}H]choline (lanes 2, 6), [^{3}H]choline (lane 4), or 10-ASA plus [^{3}H]inositol (lanes 3, 7). Incubation times were the same as in **a**. [^{3}H]choline was incubated for 20h. Cells were either ultraviolet (UV)-irradiated (lanes 1–4) or kept in the dark (lanes 5–7). Photolabelled proteins were resolved by SDS–PAGE (6–15%, Tris-Tricine) and visualized by fluorography. Identical amounts of radioactivity crosslinked to protein were applied in lanes 1 and 2; lanes 5 and 6 contain the same amounts of non-crosslinked sample. Lane 4 contains the same amount of total radioactivity as lane 2. The exposure time for lanes 3 and 7 was ten times longer than for the other lanes to compensate for the low incorporation of [^{3}H]inositol into photo-PI (**a**). Arrow, 35K band labelled with photocholesterol, photo-PC and photo-PI; arrowhead, 30K band specifically labelled with photo-PC; bracket, the major specifically cholesterol-labelled band (caveolin/VIP21; **c**). **c**, Identification of photocholesterol-labelled caveolin/VIP21. A detergent extract of [^{3}H]photocholesterol-labelled MDCK cells (Total) was subjected to immunoprecipitation using antibodies against a control antigen or caveolin/VIP21. Proteins were resolved by SDS–PAGE (6–15%, Tris-Tricine) and visualized by fluorography. The bracket shows the position of immunoprecipitated caveolin/VIP21. The difference between the M_r value for this protein and the reported apparent M_r of caveolin/VIP21 of 21K (ref. 12) is due to the Tris-Tricine gradient gel system used; these bands migrated at 22–24K in a normal Laemmli-type gel system (data not shown).

(Fig. 3b, compare lanes 1, 5), and labelled proteins were almost exclusively found in the cellular membranes (data not shown).

Although the distinct pattern of proteins labelled with [^{3}H]photocholesterol indicated specific interactions leading to the labelling, it could not be excluded that labelling with [^{3}H]photocholesterol also reflected an unspecific interaction with any type of membrane lipid. To identify the specifically cholesterol-interacting proteins, it was necessary to compare the pattern of [^{3}H]photocholesterol labelling with that obtained by photolabelling with a membrane lipid that is a major component of all cellular membranes. Phospholipids, especially the abundant phosphatidylcholine, would be suitable for that purpose. To generate phospholipid analogues suitable for photoaffinity labelling in live cells, we took advantage of the cellular biosynthetic apparatus (Fig. 1b). Cells were grown for 20h in the simultaneous presence of the non-radioactive fatty-acid analogue 10-azi stearic acid (10-ASA) (which bears the same photoactivatable carbene-generating azi group as [^{3}H]photocholesterol) and of [^{3}H]choline or [^{3}H]inositol. 10-ASA should be taken up by the cells, giving rise to photoactivatable phospholipids. The only radioactive lipids generated by the cells incubated in the presence of 10-ASA plus [^{3}H]choline and 10-ASA plus [^{3}H]inositol were [^{3}H]phosphatidylcholine and [^{3}H]phosphatidylinositol, respectively (Fig. 3a). Hence, photolabelling of a protein upon ultraviolet irradiation should reflect its interaction with photoactivatable phosphatidylcholine or phosphatidylinositol, referred to as photo-PC and photo-PI, respectively.

Labelling with photo-PC and photo-PI was dependent on ultraviolet irradiation (Fig. 3b, compare lanes 2, 3 with 6, 7) and on the presence of the photoactivatable fatty acid 10-ASA (Fig. 3b, compare lanes 2, 4). Certain proteins, such as a major band of relative molecular mass 35,000 (M_r 35K; Fig. 3b, lanes 1–3, arrow), showed relatively similar labelling with photocholesterol, photo-PC and photo-PI (that is, for each photoactivatable lipid the band contained the same proportion of the total protein-incorporated label). Photolabelling of these proteins possibly reflected their spatial proximity to the lipid probes. Labelling of some other proteins was relatively stronger with one (or two) of the three photoactivatable lipids than with the other one(s). This specific photolabelling was likely to reflect a specific protein–lipid interaction. For example, a 30K band was specifically labelled with photo-PC (Fig. 3b, lane 2, arrowhead); this band co-fractionated with mitochondria and presumably is subunit III of cytochrome oxidase (C.T., unpublished observations), which contains a specifically bound phosphatidylcholine molecule[15]. An 18K band was labelled strongly with photocholesterol (Fig. 3b, lane 1, bracket) but only weakly with photo-PC (Fig. 3b, lane 2) and photo-PI (Fig. 3b, lane 3); immunoprecipitation showed that this band was caveolin/VIP21 (Fig. 3c).

The neuroendocrine cell line PC12 is an established model system for the study of the biogenesis of neurosecretory vesicles[16,17]. To study the role of interactions between cholesterol and membrane proteins in neurosecretory-vesicle biogenesis, we labelled PC12 cells with photocholesterol, photo-PC and photo-PI. As well as comparing the pattern generated by the individual photoactivatable lipids, we took advantage of the PC12 cell subclone 27, which lacks the neuroendocrine phenotype[18]; that is, this subclone is unable to form secretory granules and SLMVs and lacks neuroendocrine marker proteins such as the granins, synaptophysin and synaptobrevin/VAMP2. Any difference in labelling between the normal PC12 cell clone 251 and the subclone 27 should therefore indicate a protein involved in neuroendocrine function.

As was the case for MDCK cells, neither PC12 cell clone metabolized [^{3}H]photocholesterol under our experimental conditions (Fig. 4a, left). Upon incubation for 20h in the presence of 10-ASA plus [^{3}H]choline or 10-ASA plus [^{3}H]inositol, both PC12 cell clones efficiently generated photo-PC and photo-PI, respectively (Fig. 4a, right).

Photo-PC and photo-PI labelling of PC12 cells resulted in very similar patterns (Fig. 4b, lanes 2, 3, 5, 6), which also showed striking similarity to those observed in MDCK cells (Fig. 3b, lanes 2, 3). As

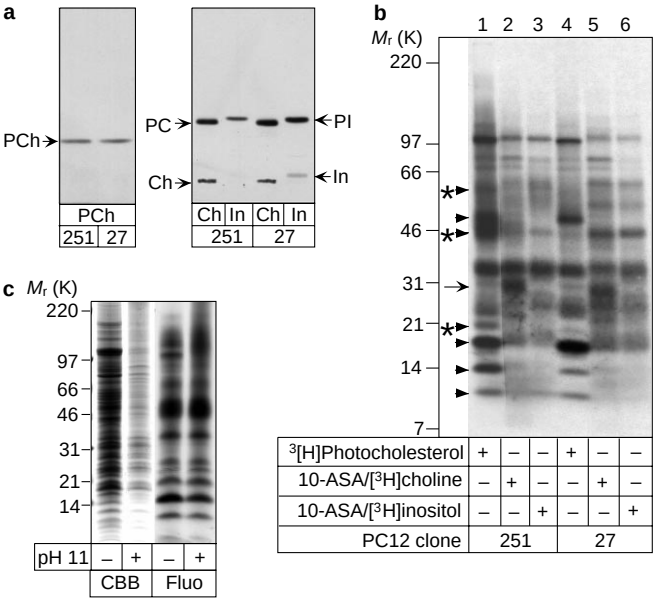

Figure 4 **Photoaffinity labelling of PC12 clone 251 and clone 27 cells.** **a**, TLC analysis of radioactive photoactivatable lipids. PC12 clone 251 (251; normal neuroendocrine phenotype) and clone 27 (27; loss of neuroendocrine phenotype) cells were grown in the presence of [^{3}H]photocholesterol (PCh, incubation time 4 h), 10-ASA plus [^{3}H]choline (Ch, 20 h) or 10-ASA plus [^{3}H]inositol (In, 20 h). Detergent extracts were resolved on TLC plates followed by fluorography. The positions of co-migrating standards (PC, phosphatidylcholine; PI, phosphatidylinositol) are denoted by arrows. **b**, Some photocholesterol-labelled proteins are neuroendocrine specific. PC12 clone 251 (lanes 1–3) and clone 27 (lanes 4–6) cells were grown (for same incubation times as in **a**) in the presence of [^{3}H]photocholesterol (lanes 1, 4), 10-ASA plus [^{3}H]choline (lanes 2, 5), or 10-ASA plus [^{3}H]inositol (lanes 3, 6), and were then UV-irradiated. Photolabelled proteins were resolved by SDS–PAGE (6–15%, Tris-Tricine) and visualized by fluorography. Similar amounts of crosslinked radioactivity were applied. Arrowheads indicate proteins that specifically bind photocholesterol as compared to photoglycerophospholipids (compare lane 1 with lanes 2, 3); amongst these (but not amongst the glycerophospholipid-binding proteins) are some (asterisks) that are specific to PC12 clone 251 versus clone 27 cells (compare lanes 1, 4). Arrow, 30K band specifically labelled with photo-PC. **c**, Photocholesterol labels a specific set of membrane proteins that are distinct from the major Coomassie-stained membrane proteins. A membrane fraction of PC12 clone 251 cells labelled with [^{3}H]photocholesterol was either left untreated (–) or extracted with sodium carbonate at pH 11 (+). Membrane proteins were resolved by SDS–PAGE (6–15%, Tris-Tricine) and visualized by CBB staining (CBB) and fluorography (Fluo).

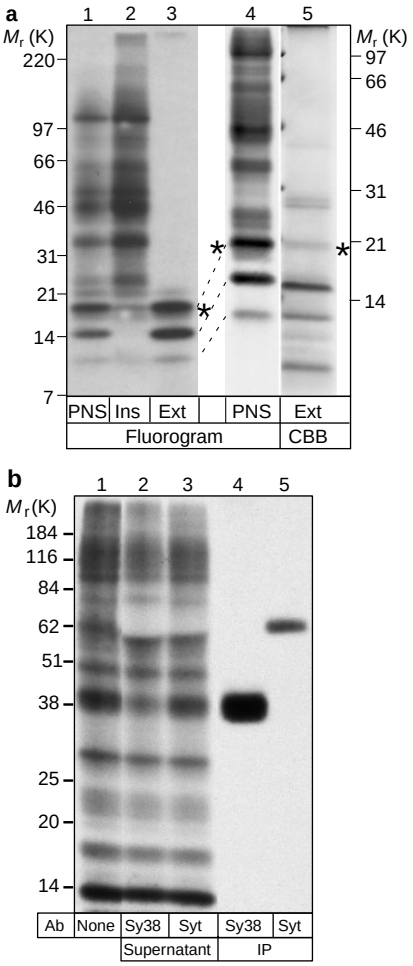

Figure 5 **Identification of photocholesterol-labelled proteins of PC12 clone 251 cells. a**, Identification of the vesicular proton ATPase (V-ATPase) 17K proteolipid subunit (c subunit). PC12 clone 251 cells were photoaffinity-labelled with [^{3}H]photocholesterol. A postnuclear supernatant (PNS; lane 1) was prepared and subjected to chloroform extraction, yielding an insoluble pellet (Ins; lane 2, containing twice the starting material of lane 1) and a chloroform extract (Ext; lane 3, containing twice the starting material of lane 1). A delipidated chloroform extract from unlabelled cells was prepared (Ext; lane 5) and co-electrophoresed with photocholesterol-labelled PNS (lane 4), and the protein band (lane 5, asterisk) corresponding to the photolabelled band at 17K (lanes 3, 4, asterisks) was identified by mass spectrometry as the c subunit of the V-ATPase. Note that the samples shown in lanes 1–3 were electrophoresed using a gel system (6–15% Tris-Tricine) different from that in lanes 4 and 5 (13% Laemmli), resulting in a slightly different electrophoretic mobility. Corresponding bands in lanes 3 and 4 are connected by dashed lines. Lanes 1–4, fluorogram; lane 5, CBB stain. **b**, Identification of synaptophysin and synaptotagmin. PC12 clone 251 cells were photolabelled with [^{3}H]photocholesterol. A detergent extract of a PNS-derived total membrane fraction was subjected to immunoprecipitation using antibodies (Ab) against synaptophysin (Sy38) and synaptotagmin (Syt). Aliquots of non-immunoprecipitated total extract (lane 1), the supernatants after immunoprecipitation (lanes 2, 3) and the immunoprecipitates (IP, lanes 4, 5, containing ten times more material than lanes 1–3) were subjected to SDS–PAGE (11% Laemmli) followed by fluorography.

observed in MDCK cells, both PC12 cell clones showed the 30K band that was labelled by photo-PC (Fig. 4b, lanes 2, 5, arrow) but not photo-PI (Fig. 4b, lanes 3, 6). Some of the photo-PC- and photo-PI-labelled bands were also labelled by photocholesterol (Fig. 4b, lanes 1, 4), but photocholesterol also specifically labelled several bands that were only weakly labelled (if at all) with photo-PC and photo-PI (Fig. 4b, lane 1, arrowheads). Although the photo-PC- and photo-PI-labelled bands were very similar between the two PC12 cell clones, at least three of the specifically photocholesterol-labelled bands in clone 251, that is the 60K, ~43K and 21K bands (Fig. 4b, lane 1, asterisks), were lacking in the neuroendocrine-deficient clone 27 (Fig. 4b, lane 4). No specifically photocholesterol-labelled band present in clone 27 but not clone 251 was detected.

The observation that certain proteins of clone 251 cells were photolabelled strongly with photocholesterol but only weakly with photo-PC indicated that the photocholesterol labelling of these proteins did not simply reflect their abundance. To corroborate this conclusion, we analysed a total membrane fraction from a post-nuclear supernatant (PNS), either untreated or after removal of peripheral membrane proteins by stripping with pH 11 carbonate, and compared the pattern of Coomassie brilliant blue (CBB)-stained protein bands with that of photocholesterol-labelled bands (Fig. 4c). The major photocholesterol-labelled bands did not correspond to the major protein bands.

Synaptic-vesicle membrane proteins specifically bind cholesterol. Three of the specifically photocholesterol-labelled proteins in both

PC12 cell clones (M_r values 17K, 14K and 10K; Fig. 4b, lane 1, arrowheads without asterisks) were found to be chloroform-soluble membrane proteins (Fig. 5a, lane 3). Chloroform solubility is a characteristic feature of the 17K proteolipid (c) subunit of the vesicular proton ATPase (V-ATPase)[19]. To identify the 17K photocholesterol-labelled band, we subjected the proteins of a delipidated chloroform/methanol extract of PC12 clone 251 cells to SDS–polyacrylamide gel electrophoresis (PAGE). The CBB-stained band (Fig. 5a, lane 5, asterisk) corresponding to the 17K radiolabelled band (Fig. 5a, lanes 3, 4, asterisks) was subjected to mass spectrometry after in-gel tryptic digestion. We identified two peptides of V-ATPase c (residues 6–36 and 37–54), which covered 32% of its amino-acid sequence, confirming that the 17K band was indeed V-ATPase c[19]. The chloroform-soluble photocholesterol-labelled bands at 14K and 10K are probably products of the degradation of the 17K V-ATPase c. The abundance of the 14K band increased upon incubation of PC12 cell detergent extracts, concomitant with a decrease in the abundance of the 17K V-ATPase c band (compare Fig. 5a, lane 1, which is a PNS directly subjected to SDS–PAGE, with Fig. 5b, lane 1, which is a PNS that had been incubated for 16h at 4°C before SDS–PAGE).

SLMVs contain the membrane protein synaptophysin[20], whose relative molecular mass is similar to that of the ~43K photocholesterol-labelled protein (Fig. 4b, lane 1, asterisk). In addition, we suspected the photocholesterol-labelled protein of M_r 60K (Fig. 4b, lane 1, asterisk) to be synaptotagmin[20], a neuroendocrine-specific protein which, in PC12 cells, is present in both SLMVs and secretory granules[21]. Immunoprecipitation confirmed the identity of the 60K and ~43K photocholesterol-labelled proteins as synaptotagmin (Fig. 5b, lane 5) and synaptophysin (Fig. 5b, lane 4), respectively.

When we separated SLMVs of photocholesterol-labelled PC12 clone 251 cells from their donor membranes — plasma membrane[22] and early endosomes[23] — by velocity glycerol-gradient centrifugation[17], photocholesterol-labelled synaptophysin (Fig. 6a, top) showed a very similar distribution to immunoreactive synaptophysin across the gradient (Fig. 6a, bottom), being found in both SLMV- and donor-membrane-containing fractions. Three other photocholesterol-labelled proteins (with M_r values of ~120K, 24K and 14K) were also detected in SLMVs (Fig. 6a, top, fractions 7–10). The lack of obvious detectability of photocholesterol-labelled synaptotagmin in SLMVs probably reflects both its lower level of labelling with photocholesterol as compared with synaptophysin at the level of whole cells (Fig. 4b, lane 1), and its broader subcellular distribution (in comparison to synaptophysin) in organelles other than SLMVs, that is, secretory granules[21].

We labelled PC12 clone 251 cells with photocholesterol and photo-PC and compared the pattern of labelled bands in a subcellular fraction enriched in SLMV donor membranes (plasma membrane and early endosomes) but largely devoid of nuclear envelope, endoplasmic reticulum, Golgi, late endosomes, lysosomes, secretory granules and mitochondria. Although, for many bands in this fraction, the labelling with photocholesterol (Fig. 6b, solid line) and photo-PC (Fig. 6b, dashed line) was relatively similar, a 17K band (Fig. 6b, arrow), corresponding to V-ATPase c, and a ~43K band (Fig. 6b, arrowhead), corresponding to synaptophysin, were significantly more strongly labelled with photocholesterol than with photo-PC. As the membranes analysed, although rich in cholesterol, contain high levels of phosphatidylcholine, the relatively stronger labelling of these proteins with photocholesterol than with photo-PC indicates their specific cholesterol binding rather than simply their residence, at high abundance, in cholesterol-rich membranes.

To investigate whether specific binding of cholesterol to synaptophysin also occurred in synaptic vesicles, we labelled intact rat brain synaptosomes, stimulated with α-latrotoxin to promote exocytosis–endocytosis, with photocholesterol and purified synaptic vesicles from the labelled synaptosomes. Synaptophysin (Fig. 6c, arrows) was the most strongly photocholesterol-labelled band, even considering the fact that this protein is the major CBB-stained band of synaptic vesicles[20]. Other labelled proteins included synaptotagmin (Fig. 6c, brackets) and a 16K band that probably represents V-ATPase c (Fig. 6c, dot). We detected no photocholesterol labelling of the transmembrane protein synaptobrevin/VAMP, which, on a molar basis, is as abundant as synaptophysin[20]. Even if the different number of transmembrane domains (synaptophysin has four such domains and syn-

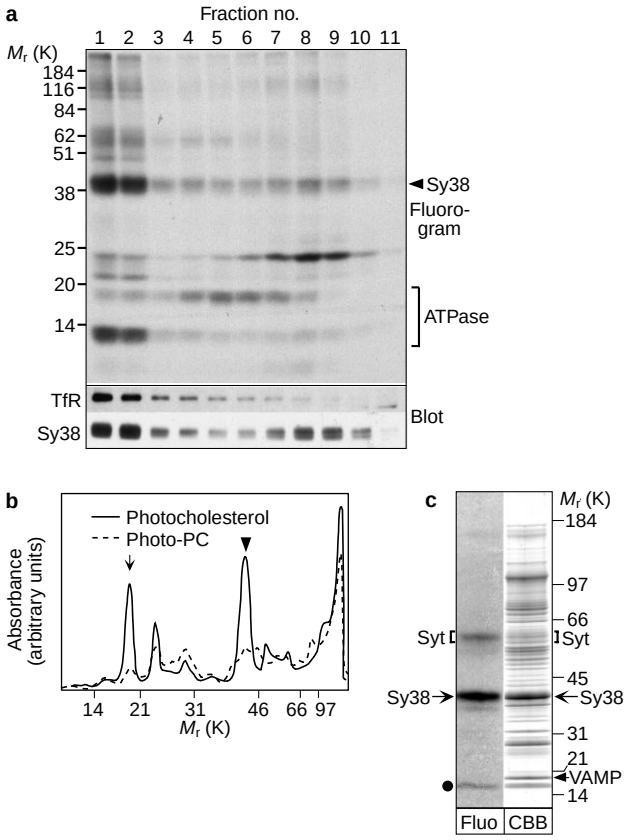

Figure 6 **Specific cholesterol binding to synaptophysin in SLMVs/synaptic vesicles and their donor membranes. a**, Photocholesterol-labelled synaptophysin is found in SLMVs. PC12 clone 251 cells were photoaffinity-labelled with [^{3}H]photocholesterol. A 53,000*g* supernatant was prepared and subjected to velocity glycerol-gradient centrifugation. Gradient fractions were subjected to SDS–PAGE (12% Laemmli) followed by fluorography (Fluorogram) or immunoblotting (Blot) for transferrin receptor (TfR) and synaptophysin (Sy38). The peak of synaptophysin immunoreactivity in fractions 7–10, which are largely devoid of transferrin receptor, represents SLMVs. Arrowhead, synaptophysin (Sy38); bracket, 17K and 14K forms of the c subunit of V-ATPase. Both the 17K and the 14K form of V-ATPase c subunit are found in SLMV-containing fractions; however, whereas most of the 14K form, like the majority of synaptophysin, is found in fractions 1 and 2, which contain endosomes, the majority of the 17K form is found in membranes that sediment slightly faster than SLMVs. Fraction 1, bottom of the gradient; fraction 11, top of the gradient. **b**, Specific labelling by photocholesterol in a membrane fraction enriched in plasma membrane and endosomes. A subcellular fraction enriched in plasma membrane and endosomes of PC12 clone 251 cells labelled with [^{3}H]photocholesterol (solid line) or photo-PC (dashed line) was prepared by sequential sucrose velocity and equilibrium centrifugation. Membrane proteins were resolved by SDS–PAGE (12% Laemmli) and visualized by fluorography. Fluorograms were quantified by densitometric scanning. Arrow, V-ATPase c subunit; arrowhead, synaptophysin. **c**, Photocholesterol labels synaptophysin but not synaptobrevin/VAMP in synaptic vesicles. Intact rat brain synaptosomes were incubated for 25min with [^{3}H]photocholesterol in the presence of α-latrotoxin and then UV-irradiated. Synaptic vesicles were purified and proteins were analysed by SDS–PAGE (7.5–15%, Laemmli) followed by CBB staining and fluorography. Brackets, synaptotagmin (Syt); arrows, synaptophysin (Sy38); arrowhead, synaptobrevin/VAMP (VAMP) (see ref. 44); dot, a photocholesterol-labelled 16K protein, presumably V-ATPase c. Note the absence of labelling of synaptobrevin/VAMP.

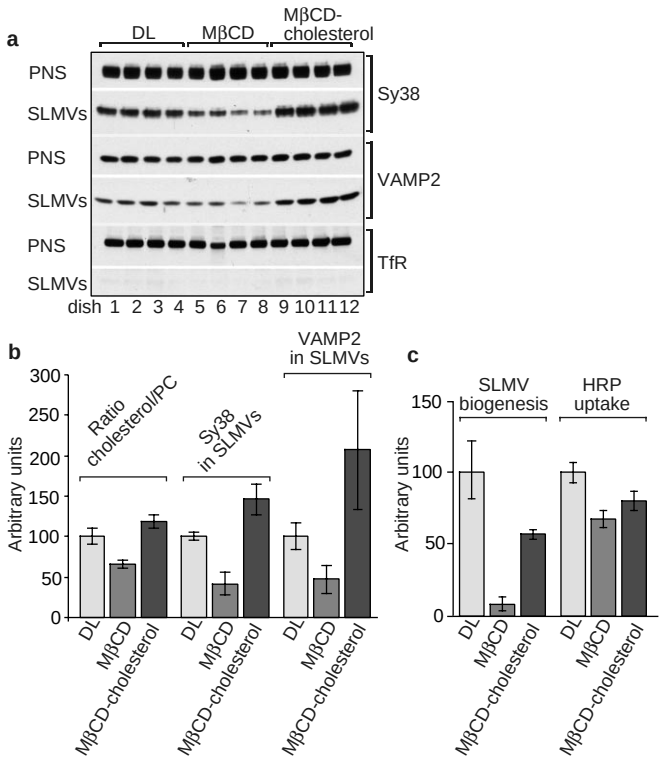

Figure 7 **The effect of cholesterol depletion and replenishment on PC12 cell SLMVs. a**, **b**, Manipulation of cellular cholesterol influences SLMV levels. **a**, PC12 clone 251 cells were treated for 45 min with delipidated medium containing either no addition (DL), 5 mg ml^{-1} MβCD (MβCD), or 2.5 mg ml^{-1} MβCD plus 2.5 mg ml^{-1} MβCD–cholesterol complex (MβCD-cholesterol). A PNS (PNS, 1/150 of total) and a fraction enriched in SLMVs (SLMVs, 1/20 of total) were prepared. Proteins were resolved by SDS–PAGE; synaptophysin (Sy38), synaptobrevin/VAMP2 (VAMP2) and transferrin receptor (TfR) in the PNS and SLMVs were visualized by immunoblotting; for each antibody, PNS and SLMVs received the same exposure. Results from quadruplicate dishes are shown. **b**, The ratio of cholesterol to phosphatidylcholine (PC) was determined in the 55,000*g* membrane pellet of cells treated as described in **a**. The levels of synaptophysin (Sy38) and synaptobrevin/VAMP2 in SLMVs, expressed relative to those found in the PNS, were determined from the blots shown in **a**. The values obtained under control conditions (DL) were set to 100 and the values obtained for the other conditions were expressed relative to the control. Data are the means ± s.d. of quadruplicate determinations and are representative of at least three experiments. **c**, Differential effects of MβCD treatment on SLMV biogenesis and total endocytic activity of PC12 cells. For analysis of SLMV biogenesis, PC12 clone 251 cells were biotinylated for 30 min at 18 °C, treated for 10 min at 18 °C with delipidated medium containing no addition (DL), 5 mg ml^{-1} MβCD (MβCD), or 2.5 mg ml^{-1} MβCD plus 2.5 mg ml^{-1} MβCD–cholesterol complex (MβCD–cholesterol), and chased in the respective media for 15 min at 37 °C. For analysis of HRP uptake, the same protocol was used except that the biotinylation step was omitted and HRP was present during the chase at 37 °C. SLMV biogenesis was determined from the appearance of biotinylated synaptophysin in SLMVs, expressed relative to that found in the PNS. Total cellular HRP uptake was quantified to determine the total endocytic activity. The values obtained under control conditions (DL) were set to 100 and the values obtained under the other conditions were expressed relative to the control. Data are the means ± s.d.; SLMV biogenesis, $n = 3$; HRP uptake, $n = 6$.

aptobrevin/VAMP has one) is taken into account, synaptobrevin/VAMP should have incorporated detectable levels of photocholesterol if this labelling were simply a reflection of the abundance of transmembrane domains in a cholesterol-rich membrane. We conclude that the labelling of synaptophysin with photocholesterol reflects synaptophasin's specific interaction with cholesterol.

Steady-state amounts of SLMVs correlate with cellular cholesterol levels. To study a possible role of the binding of SLMV membrane proteins to cholesterol in the SLMV life cycle, we manipulated cholesterol levels of PC12 clone 251 cells by extraction with MβCD, followed by subcellular fractionation[17,24] and analysis of the SLMV marker proteins synaptophysin and synaptobrevin/VAMP2 (ref. 20) and of transferrin receptor, a marker of the plasma membrane and of endosomal compartments[25] (Fig. 7a).

Control cells were treated for 45 min with delipidated medium (Fig. 7a, b, DL). These cells showed a distribution of synaptophysin between SLMVs and plasma membranes/endosomes that was similar to that of cells grown in the continuous presence of serum lipids (data not shown). Cholesterol was depleted to 60–70% of control values by a 45-min treatment with 5 mg ml^{-1} (3.8 mM) MβCD in delipidated medium (Fig. 7a, b, MβCD). As a control for the effect of MβCD, cells were treated for 45 min with 2.5 mg ml^{-1} MβCD plus 2.5 mg ml^{-1} MβCD–cholesterol complex in delipidated medium (Fig. 7a, b, MβCD–cholesterol). The latter treatment, which exposed the cells to the same concentration of MβCD as that to which the cholesterol-depleted cells were exposed but left the cholesterol levels unchanged or even slightly increased as compared with control cells grown in delipidated medium (Fig. 6b), served as a control for any effects of MβCD other than cholesterol depletion. MβCD treatment reduced the amount of synaptophysin in SLMVs to 40% of control cell levels (Fig. 7a, b). We observed significantly increased amounts of synaptophysin in SLMVs after MβCD–cholesterol treatment, showing that changes in cholesterol levels, and not the presence of MβCD *per se*, caused the effect on this SLMV marker protein. Higher concentrations of MβCD (15–20 mg ml^{-1}) caused the complete disappearance of synaptophysin from SLMVs (data not shown) but also resulted in general changes in cell morphology, so unspecific effects could not be excluded. The behaviour of synaptobrevin/VAMP2 was similar to that of synaptophysin (Fig. 7a, b). This parallel behaviour of two SLMV membrane proteins made it likely that the reduction in their amounts in the SLMV-containing fraction reflected a decrease in SLMV levels rather than their impaired targeting to SLMVs.

Limited cholesterol depletion blocks SLMV biogenesis but not total endocytic activity. To study the mechanism underlying the reduction in SLMV levels upon cholesterol depletion, we measured the biogenesis of SLMVs from the plasma-membrane donor compartment, using a pulse–chase protocol[24]. Cells were biotinylated at 18 °C and afterwards sequentially chased at 18 °C and 37 °C using media as above to manipulate cellular cholesterol levels during the chase periods. The amount of biotinylated synaptophysin incorporated into SLMVs during the 37 °C chase was quantified and used to calculate the extent of SLMV biogenesis. Upon MβCD-induced cholesterol reduction to 80% of control values (data not shown), we observed a >90% reduction in SLMV biogenesis (Fig. 7c, compare DL with MβCD). The effect of MβCD treatment on SLMV biogenesis was much less pronounced if half of the MβCD was loaded with cholesterol (Fig. 7c, compare MβCD with MβCD–cholesterol). To clarify whether the dependence on cholesterol is specific for SLMV biogenesis or is a general feature of endocytosis, we compared SLMV biogenesis with fluid-phase uptake of horseradish peroxidase (HRP) as a marker of the total endocytic activity. MβCD treatment caused only a moderate decrease in HRP uptake (Fig. 7c, compare DL with MβCD). Most of this decrease was also observed when cells were treated with MβCD–cholesterol (Fig. 7c), indicating that most of the effect of MβCD treatment on HRP uptake was caused not by cholesterol depletion but by MβCD itself. We conclude that the biogenesis of SLMVs is more sensitive to cholesterol reduction than is the activity of other endocytic pathways.

Discussion

We have shown that lipid photoaffinity labelling is a useful tool with which to detect protein–lipid interactions *in vivo*. Several lines of evidence indicate that photocholesterol behaves like cholesterol. These include the incorporation of photocholesterol into DICs and

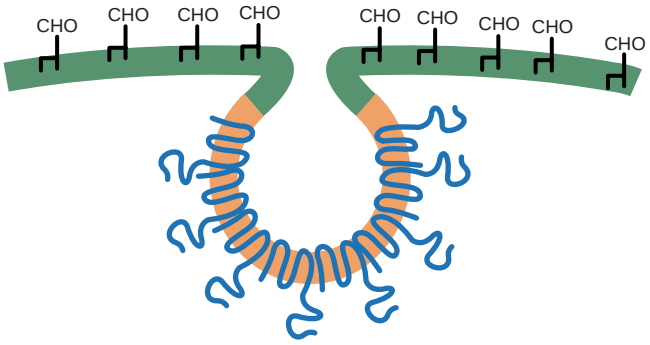

Figure 8 **Cholesterol–synaptophysin interaction and the biogenesis of SLMVs.** In the plasma membrane (green), cholesterol is associated with glycosphingolipids (CHO). In the membrane of the forming SLMV (orange), cholesterol is associated with oligomeric cholesterol-binding proteins such as synaptophysin (blue). The latter association may promote membrane curvature and hence support SLMV biogenesis.

the specific photocholesterol labelling of apolipoproteins and of the membrane protein caveolin/VIP21, which is known to bind cholesterol *in vitro*[13]. It is, therefore, highly likely that labelling of proteins by photocholesterol reflects their physiological interaction with cholesterol.

For *in vivo* photolabelling with glycerophospholipids, we developed a new approach that exploits the cellular biosynthetic apparatus to generate photoactivatable radioactive phospholipids *in vivo*. We added the photoactivatable fatty acid 10-ASA to the culture medium. 10-ASA did not bear radioactivity, as this would have led to massive photolabelling by the free fatty acid and also by fatty-acid-containing compounds such as acyl-CoAs and acyl-carnithines. Instead, we added non-radioactive 10-ASA together with the radioactive phospholipid head groups choline or inositol. A radioactive photoactivatable compound was then generated by the biosynthetic apparatus and was restricted to phosphatidylcholine and phosphatidylinositol, respectively. This strategy ensures correct targeting of the photolabel, because the *in vivo*-synthesized phospholipids will follow the normal pathways of intracellular lipid targeting.

Cholesterol–protein interactions are a recurring motif in the late endomembrane system. A comparison of the patterns generated by photo-PC and photo-PI in the three cell lines analysed showed remarkably few differences, whereas significant differences were detected between the patterns generated by photocholesterol and by photo-PC or photo-PI. Further analysis showed that these differences were mainly due to the presence of proteins that play a part in the specialized membrane traffic typical of the respective cell line: major specifically photocholesterol-labelled proteins in PC12 clone 251 cells (synaptophysin, synaptotagmin and V-ATPase c) and MDCK cells (caveolin/VIP21) function in regulated secretion and maintenance of epithelial polarity, respectively. Our overall impression is that proteins that interact with phospholipids are involved in 'housekeeping' functions, whereas proteins that interact with cholesterol are associated with specialized post-Golgi membrane function and traffic. The localization of photocholesterol-labelled proteins to membranes with a high cholesterol content, such as endosomes[26] and SLMVs[27], is not sufficient to explain why these proteins are only weakly labelled with glycerophospholipid analogues. All of these membranes still contain substantial (~60% on a molar basis) amounts of phospholipids, with phosphatidylcholine usually being the predominant phospholipid. Thus specific labelling with photocholesterol but not with phosphatidylcholine or phosphatidylinositol does not reflect the lipid composition of the environment but rather the affinity and binding capacity of the labelled proteins for cholesterol. In support of this conclusion, analysis of purified synaptic vesicles revealed selective photocholesterol binding to some, but not all, transmembrane proteins, with synaptophysin being labelled to a significantly greater extent than would be expected from the abundance of its transmembrane domains relative to the other synaptic-vesicle transmembrane proteins.

What are the functions of a specific protein–cholesterol interaction? Although V-ATPase might require cholesterol for its pumping activity[28], the function of the other major labelled proteins, especially synaptophysin and caveolin/VIP21, is only partially understood and it seems reasonable to assume that cholesterol binding is part of their physiological role. Furthermore, all three — synaptophysin, caveolin/VIP21 and the V-ATPase — are present in at least hexameric[19,29] or even higher oligomeric[30] form. The combination of specific cholesterol-binding and oligomerizing properties should allow these proteins to function in the mutual enrichment of proteins and lipids to form distinct membrane microdomains. The microdomains formed by these proteins and cholesterol are likely to be curved, as all three proteins are usually found in highly curved structures such as endosomes, synaptic vesicles and caveolae.

The membranes of synaptic vesicles contain high amounts of cholesterol[27] and, as shown here, several cholesterol-interacting proteins. Both the size of the steady-state SLMV pool and SLMV biogenesis were markedly affected by cholesterol depletion. In comparison with the effects of cholesterol depletion on transferrin-receptor endocytosis[31,32], the effect on SLMV biogenesis was already much more marked at significantly lower concentrations of the depleting agent, MβCD. The total endocytic activity of PC12 cells was only weakly affected by our conditions of cholesterol depletion, indicating that the strong dependence on cholesterol may be a specific feature of SLMV biogenesis compared with other endocytic pathways.

What is the molecular basis of the cholesterol dependence of SLMV formation? Cholesterol dependence of other membrane-trafficking events reflects the involvement of detergent-insoluble cholesterol/sphingolipid-based membrane rafts[33,34]. Two pieces of evidence run counter to the view that the SLMV is such a raft-based organelle. First, although high in cholesterol, the SLMV membrane is low in sphingolipids, particularly in glycosphingolipids[27]. Second, synaptophysin, a major cholesterol-interacting protein in PC12 cells and also a major membrane protein of PC12 cell SLMVs[17], is not insoluble in Triton X-100 (ref. 35). We favour an alternative explanation for the cholesterol dependence of SLMV formation. Cholesterol and cholesterol-interacting transmembrane proteins associate in the SLMV donor compartment to support the formation of SLMVs (Fig. 8). Cholesterol deprivation prevents this association and impairs SLMV formation, probably by inhibiting the induction of curvature of the forming bud, as suggested for the clathrin-coated endocytic vesicle[31,32]. We propose that association of cholesterol with oligomerizing membrane proteins is a mechanism that is important for the formation of highly curved structures such as SLMVs and caveoli. The presence of other oligomerizing four-transmembrane-domain proteins in highly curved post-*trans*-Golgi-network transport vesicles (SCAMP proteins)[36,37] or the rims of the photoreceptor discs (RDS/peripherin)[38,39] indicates that this may be a general way by which curved structures can be formed. □

Methods

For more detailed methods, see Supplementary Information.

Chemical syntheses.

Photocholesterol was synthesized by conversion of 6-keto-5α-cholestan-3β-ol (Sigma) to 6-azi-5α-cholestan-3β-ol (ε=70 at 354 nm; ε=64 at 371 nm; 2.8 mg ml^{-1} in ethyl acetate), following the method of ref. 40. Photocholesterol was oxidized to 6-azi-5α-cholestan-3-on (ε=70 at 354 nm; ε=62 at 371 nm; 2.7 mg ml^{-1} in ethyl acetate; m/z=413) using chromic acid and subsequently reduced to [^{3}H]photocholesterol ([3α-^{3}H]6-azi-5α-cholestan-3β-ol, ~6 Ci mmol^{-1}) using [^{3}H]$NaBH_4$. Unlabelled photocholesterol was verified by mass spectrometry of its sulphate ester.

10-azi-stearic acid (10-ASA; ε=56 at 350 nm; 3.1 mg ml^{-1} in methanol) was synthesized from 10-keto-stearic acid following the method of ref. 40, transferred into serum as described[41], and used for cell labelling at ~50 μM.

Photoaffinity labelling.

Human plasma (100 μl) was incubated for 15 min at 37 °C with 10 μCi [^{3}H]photocholesterol and irradiated for 10 min at 4 °C using the filtered (λ>310 nm) beam of a high-pressure mercury lamp[42]; apolipoprotein A1 and apolipoprotein B were immunoprecipitated and then analysed by SDS–PAGE (5–

15% gradient gel) and fluorography.

Rat brain synaptosomes (P2′) were isolated as described[43] and incubated for 25 min at 37 °C in oxygenated Krebs–Ringer buffer containing [^{3}H]photocholesterol–MβCD complex (200 µl per 10 ml synaptosome suspension), with addition of 1 nM α-latrotoxin after 5 min and of 1.5 mM $CaCl_2$ after 15 min (to enhance incorporation of photocholesterol into synaptic vesicles by stimulating exocytosis–endocytosis), followed by ultraviolet irradiation at 4 °C for 17 min. Synaptic vesicles were purified from the labelled synaptosomes through the sucrose equilibrium centrifugation step (SG-V) as described[43] and subjected to SDS–PAGE (7.5–15% gradient) followed by CBB staining and fluorography. Proteins were identified by comparison of the CBB-stained gel with the nearly identical pattern shown in ref. 44. Results identical to those shown in Fig. 6c were obtained when 1.5 mM $CaCl_2$ was added to the synaptosome suspension before the incubation with [^{3}H]photocholesterol–MβCD complex and α-latrotoxin; in this case, the suspension was irradiated after 10 min of α-latrotoxin treatment (data not shown).

PC12 clone 251C (refs 16, 45), PC12 clone 27 (ref. 18) and MDCK[46] cells were incubated for 4–16 h in lipid-free medium containing either [^{3}H]photocholesterol–MβCD complex (100 µl per 2 ml medium, 400 µl per 20 ml) or 10-ASA (100 µl per 3 ml) plus [^{3}H]choline (200 µCi per 3 ml) or [^{3}H]inositol (200 µCi per 3 ml), and ultraviolet-irradiated for 20 min at room temperature on the dish. Postnuclear extracts were analysed by SDS–PAGE/fluorography and TLC/fluorography.

Identification of V-ATPase c.

A chloroform extract was prepared from total PNS membranes of PC12 clone 251 cells; the extract was delipidated as described[47] and subjected to SDS–PAGE. The protein band corresponding to the [^{3}H]photocholesterol-labelled chloroform-soluble 17K protein was identified as V-ATPase c by mass spectrometry of tryptic peptides.

Effect of MβCD treatment on SLMV levels.

PC12 clone 251 cells were incubated for 45 min at 37 °C in 80 µl cm^{-2} DMEM supplemented with 15% delipidated serum and containing either no addition, 5 mg ml^{-1} (3.8 mM) MβCD, or 2.5 mg ml^{-1} MβCD plus 2.5 mg ml^{-1} MβCD–cholesterol complex (27 mg of cholesterol per gram MβCD, prepared as described[48]). SLMVs were isolated from PNS by single 30% glycerol step centrifugation[24], and analysed by immunoblotting. The 55,000*g* membrane pellet obtained before glycerol step centrifugation was used for cholesterol determination.

Effect of MβCD treatment on SLMV biogenesis and HRP uptake.

SLMV biogenesis was determined by quantifying the appearance of synaptophysin, biotinylated at the cell surface at 18 °C, in SLMVs as described[22,24], except that after biotinylation the cells were incubated for 10 min at 18 °C in the presence of MβCD or MβCD–cholesterol complex as above, followed by a 15-min chase at 37 °C in the respective fresh medium. For analysis of HRP uptake, the biotinylation step was omitted and HRP (1 mg ml^{-1}) was added at the beginning of the 37 °C incubation. HRP activity was determined in a postnuclear detergent extract.

Miscellaneous.

Oxidation of [^{3}H]photocholesterol and its 3α-epimer [3β-^{3}H]6-azi-5α-cholestan-3α-ol with cholesterol oxidase was monitored by release of tritiated water.

The [^{3}H]photocholesterol–MβCD inclusion complex[48] contained 7 mg MβCD (Sigma) and 0.4–1 mCi [^{3}H]photocholesterol in 400 µl water.

A fraction enriched in plasma membranes and endosomes was obtained by sequential velocity (fractions 1–3 of 13) and equilibrium (fraction 7 of 13) sucrose gradient centrifugation[16].

RECEIVED 19 AUGUST 1999; REVISED 16 NOVEMBER 1999; ACCEPTED 26 NOVEMBER 1999; PUBLISHED 10 DECEMBER 1999.

1. Kirchhausen, T., Bonifacino, J. S. & Riezman, H. Linking cargo to vesicle formation: receptor tail interactions with coat proteins. *Curr. Opin. Cell Biol.* **9,** 488–495 (1997).
2. Brown, D. & London, E. Functions of lipid rafts in biological membranes. *Annu. Rev. Cell Dev. Biol.* **14,** 111–136 (1998).
3. Simons, K. & Ikonen, E. Functional rafts in cell membranes. *Nature* **387,** 569–572 (1997).
4. Thiele, C. & Huttner, W. B. Protein and lipid sorting from the trans-Golgi network to secretory granules — recent developments. *Semin. Cell Dev. Biol.* **9,** 511–516 (1998).
5. Nickel, W., Bruegger, B. & Wieland, F. T. Protein and lipid sorting between the endoplasmatic reticulum and the Golgi complex. *Semin. Cell Dev. Biol.* **9,** 493–502 (1998).
6. Brown, D. A. & Rose, J. K. Sorting of GPI-anchored proteins to glycolipid-enriched membrane subdomains during transport to the apical cell surface. *Cell* **68,** 533–544 (1992).
7. Radhakrishnan, R. *et al.* Phospholipids containing photoactivable groups in studies of biological membranes. *Ann. NY Acad. Sci.* **346,** 165–198 (1980).
8. Stoffel, W., Salm, K.-P. & Mueller, M. Syntheses of phosphatidylcholines, sphingomyelins and cholesterol substituted with azido fatty acids. *Hoppe-Seylers Z. Physiol. Chem.* **363,** 1–18 (1982).
9. Stoffel, W. & Metz, P. Covalent cross-linking of photosensitive phospholipids to human serum high density apolipoproteins (apoHDL). *Hoppe-Seylers Z. Biol. Chem.* **360,** 197–206 (1979).
10. Westerman, J. *et al.* Identification of the lipid binding site of phosphatidylcholine-transfer protein with phosphatidylcholine analogs containing photoactivable carbene precursors. *Eur. J. Biochem.* **132,** 441–449 (1983).
11. Pryde, J. G. & Phillips, J. H. Fractionation of membrane proteins by temperature-induced phase separation in Triton X-114. *Biochem. J.* **233,** 525–533 (1986).
12. Kurzchalia, T. V. *et al.* VIP21, a 21-kD membrane protein is an integral component of trans-Golgi-network-derived transport vesicles. *J. Cell Biol.* **118,** 1003–1014 (1992).
13. Murata, M. *et al.* VIP21/caveolin is a cholesterol-binding protein. *Proc. Natl Acad. Sci. USA* **92,** 10339–10343 (1995).
14. Ikonen, E. Molecular mechanisms of intracellular cholesterol transport. *Curr. Opin. Lipidol.* **8,** 60–64 (1997).
15. Iwata, S., Ostermeier, C., Ludwig, B. & Michel, H. Structure at 2.8 Å resolution of cytochrome c oxidase from Paracoccus denitrificans. *Nature* **376,** 660–669 (1995).
16. Tooze, S. A. & Huttner, W. B. Cell-free protein sorting to the regulated and constitutive secretory pathways. *Cell* **60,** 837–847 (1990).
17. Clift-O'Grady, L., Linstedt, A. D., Lowe, A. W., Grote, E. & Kelly, R. B. Biogenesis of synaptic vesicle-like structures in a pheochromocytoma cell line. *J. Cell Biol.* **110,** 1693–1703 (1990).
18. Corradi, N. *et al.* Overall lack of regulated secretion in a PC12 variant cell clone. *J. Biol. Chem.* **271,** 27116–27124 (1996).
19. Finbow, M. E. & Harrison, M. A. The vacuolar H-ATPase: a universal proton pump. *Biochem. J.* **324,** 697–712 (1997).
20. Jahn, R. & Südhof, T. C. Synaptic vesicles and exocytosis. *Annu. Rev. Neurosci.* **17,** 219–246 (1994).
21. Bauerfeind, R., Jelinek, R. & Huttner, W. B. Synaptotagmin I- and II-deficient PC12 cells exhibit calcium-independent, depolarization-induced neurotransmitter release from synaptic-like microvesicles. *FEBS Lett.* **364,** 328–334 (1995).
22. Schmidt, A., Hannah, M. J. & Huttner, W. B. Synaptic-like microvesicles of neuroendocrine cells originate from a novel compartment that is continuous with the plasma membrane and devoid of transferrin receptor. *J. Cell Biol.* **137,** 445–458 (1997).
23. Lichtenstein, Y., Desnos, C., Fàundez, V., Kelly, R. B. & Clift-O'Grady, C. Vesiculation and sorting from PC12-derived endosomes in vitro. *Proc. Natl Acad. Sci. USA* **95,** 11223–11228 (1998).
24. Schmidt, A. & Huttner, W. B. Biogenesis of synaptic-like microvesicles in perforated PC12 cells. *Methods: Companion to Methods Enzymol.* **16,** 160–169 (1998).
25. Trowbridge, I. S., Collawn, J. F. & Hopkins, C. R. Signal-dependent membrane protein trafficking in the endocytic pathway. *Annu. Rev. Cell Biol.* **9,** 129–161 (1993).
26. Evans, W. H. & Hardison, W. G. Phospholipid, cholesterol, polypeptide and glycoprotein composition of hepatic endosome subfractions. *Biochem. J.* **232,** 33–36 (1985).
27. Breckenridge, W. C., Morgan, I. G., Zanetta, J. P. & Vincendon, G. Adult rat brain synaptic vesicles. II. Lipid composition. *Biochim. Biophys. Acta* **320,** 681–686 (1973).
28. Perez-Castineira, J. R. & Apps, D. K. Vacuolar H(+)-ATPase of adrenal secretory granules. Rapid partial purification and reconstitution into proteoliposomes. *Biochem. J.* **271,** 127–131 (1990).
29. Thomas, L. *et al.* Identification of synaptophysin as a hexameric channel protein of the synaptic vesicle membrane. *Science* **242,** 1050–1053 (1988).
30. Monier, S. *et al.* VIP21-caveolin, a membrane protein constituent of the caveolar coat, oligomerizes in vivo and in vitro. *Mol. Biol. Cell* **6,** 911–927 (1995).
31. Rodal, S. K. *et al.* Extraction of cholesterol with methyl-beta-cyclodextrin perturbs formation of clathrin-coated endocytic vesicles. *Mol. Biol. Cell* **10,** 961–974 (1999).
32. Subtil, A. *et al.* Acute cholesterol depletion inhibits clathrin-coated pit budding. *Proc. Natl Acad. Sci. USA* **96,** 6775–6780 (1999).
33. Keller, P. & Simons, K. Cholesterol is required for surface transport of influenza virus hemagglutinin. *J. Cell Biol.* **140,** 1357–1367 (1998).
34. Ledesma, M. D., Simons, K. & Dotti, C. G. Neuronal polarity: essential role of protein-lipid complexes in axonal sorting. *Proc. Natl Acad. Sci. USA* **95,** 3966–3971 (1998).
35. Hannah, M. J., Weiss, U. & Huttner, W. B. Differential extraction of proteins from paraformaldehyde-fixed cells: lessons from synaptophysin and other membrane proteins. *Methods: Companion to Methods Enzymol.* **16,** 170–181 (1998).
36. Brand, S. H. & Castle, J. D. SCAMP 37, a new marker within the general cell surface recycling system. *EMBO J.* **12,** 3753–3761 (1993).
37. Wu, T. T. & Castle, J. D. Evidence for colocalization and interaction between 37 and 39 kDa isoforms of secretory carrier membrane proteins (SCAMPs). *J. Cell Sci.* **110,** 1533–1541 (1997).
38. Molday, R. S., Hicks, D. & Molday, L. Peripherin. A rim-specific membrane protein of rod outer segment discs. *Invest. Ophthalmol. Vis. Sci.* **28,** 50–61 (1987).
39. Goldberg, A. F. & Molday, R. S. Subunit composition of the peripherin/rds-rom-1 disk rim complex from rod photoreceptors: hydrodynamic evidence for a tetrameric quaternary structure. *Biochemistry* **35,** 6144–6149 (1996).
40. Church, R. F. R. & Weiss, M. J. Diazirines. II. Synthesis and properties of small functionalized diazirine molecules. Some observations on the reaction of a diaziridine with the iodine-iodide ion system. *J. Org. Chem.* **35,** 2465–2471 (1970).
41. Spector, A. A. & Hoak, J. C. An improved method for the addition of long-chain free fatty acid to protein solutions. *Anal. Biochem.* **32,** 297–302 (1969).
42. Beisswanger, R. *et al.* Existence of distinct tyrosylprotein sulfotransferase genes: molecular characterization of tyrosylprotein sulfotransferase-2. *Proc. Natl Acad. Sci. USA* **95,** 11134–11139 (1998).
43. Huttner, W. B., Schiebler, W., Greengard, P. & De Camilli, P. Synapsin I (protein I), a nerve terminal-specific phosphoprotein. III. Its association with synaptic vesicles studied in a highly purified synaptic vesicle preparation. *J. Cell Biol.* **96,** 1374–1388 (1983).
44. Baumert, M., Maycox, P.R., Navone, F., De Camilli, P. & Jahn, R. Synaptobrevin: an integral membrane protein of 18,000 daltons present in small synaptic vesicles of rat brain. *EMBO J.* **8,** 379–384 (1989).
45. Heumann, R., Kachel, V. & Thoenen, H. Relationship between NGF-mediated volume increase and "priming effect" in fast and slow reacting clones of PC12 pheochromocytoma cells. *Exp. Cell Res.* **145,** 179–190 (1983).
46. Pimplikar, S., Ikonen, E. & Simons, K. Basolateral protein transport in streptolysin O-permeabilized MDCK cells. *J. Cell Biol.* **125,** 1025–1035 (1994).
47. Zacchetti, D., Peränen, J., Murata, M., Fiedler, K. & Simons, K. VIP17-MAL, a proteolipid in apical transport vesicles. *FEBS Lett.* **377,** 465–469 (1995).
48. Klein, U., Gimpl, G. & Fahrenholz, F. Alteration of the myometrial plasma membrane cholesterol content with beta cyclodextrin modulates the binding affinity of the oxytocin receptor. *Biochemistry* **34,** 13784–13793 (1995).

ACKNOWLEDGEMENTS

We thank A. Bosserhoff and R. Frank for mass spectrometry of V-ATPase c; K. Burger for help with photocholesterol synthesis; R. Sandhoff and F. Wieland for mass spectrometry of photocholesterol; A. Schmidt for advice on analysis of PC12 cell SLMVs; and P. Rosa and J. Meldolesi for PC12 clone 27 cells. This work was supported by grants from the DFG (SFB 317, C2 to W.B.H.; SFB 474 to F.F.), the EC (ERB-FMRX-CT96-0023 and ERBBIO4CT960058 to W.B.H.) and the FCI (to W.B.H.).

Correspondence and requests for materials should be addressed to C.T. or W.B.H.

Supplementary information is available on *Nature Cell Biology*'s World-Wide Web site (http://cellbio.nature.com) or as paper copy from the London editorial office of *Nature Cell Biology*.

